Machinery & Energetics
Vol. 13, No. 2. 2022

Journal homepage:
https://technicalscience.com.ua/en

UDC 622.23
DOI: 10.31548/machenergy.13(2).2022.41-49

Volodymyr Gritsyuk[1*], Igor Nevliudov[1], Mykola Zablodskiy[2], Periasami Subramanian[3]

[1]Kharkiv National University of Radio Electronics
61166, 14 Nauky Ave., Kharkiv, Ukraine

[2]National University of Life and Environmental Sciences of Ukraine
03041, 15 Heroiv Oborony, Kyiv, Ukraine

[3]Tamil Nadu Agricultural University
641003, Lawley Road, Coimbatore, India

Estimation of Eddy Currents and Power Losses in the Rotor of a Screw Electrothermomechanical Converter for Additive Manufacturing

Abstract. 3D printing technologies for large-scale structures allow architects and builders to considerably expand the design boundaries of structures and increase the efficiency of their construction. Mobile robotic platforms for 3D printing are increasingly being implemented in the construction sector, as well as in the production of road surfaces, allowing to solve the problem of limited working space. The typical design of the extruder assembly of a robotic platform for 3D printing large-scale structures can be improved by combining an electric motor, an auger extruder, and a heater in one housing. The proposed auger-type electrothermomechanical converter uses an external auger rotor, which simultaneously performs the functions of an asynchronous motor rotor, a heating element, an actuator, and a protective housing. The purpose of this study was to evaluate the efficiency of using an auger converter as part of a mobile robotic platform for additive manufacturing. For converters operating in difficult conditions, the use of field calculation methods is relevant. In this study, a field calculation was performed using the finite element method and the spatial distribution of eddy currents in the section of the hollow ferromagnetic rotor was found. Pictures of the three-dimensional distribution of the z-component, the normal component of the density of eddy currents, as well as the distribution of the dissipated power density, which considers all types of losses in the rotor, were obtained using the Comsol Multiphysics software and computing complex. The practical value of the obtained results lies in the possibility of predicting optimal indicators of the influence of the thermal regime on the material, as well as the speed of rotation of the converter rotor. This will determine the mechanical properties of the material at the output of the device

Keywords: 3D printing, mobile robotic platform, numerical calculation, external auger rotor, extruder assembly, power density

Article's History: Received: 16.12.2021; Revised: 09.03.2022; Accepted: 27.04.2022.

INTRODUCTION

3D printing is a trending technology of modern times, and its application is constantly growing, as it reduces the cost of production. Additive manufacturing provides unique advantages in creating complex structures that are in high demand in the aerospace industry [1], biomedicine [2; 3], automotive [4] and other areas [5; 6]. One of the problems with 3D printing is that typical desktop printers are stationary and have limited working space. Mobile platforms for 3D printing solve this problem, allowing to move without restrictions [7].

To increase the efficiency and cost-effectiveness of the mobile robotic platform for 3D printing technology of large-scale structures, it is proposed to improve the design of the extruder assembly by combining an electric motor, an auger extruder, and a heater in one housing. This will not only save weight and size, but also substantially increase the efficiency and reliability of the entire system.

Apart from the freedom of design, additive manufacturing has enormous potential in the construction industry, as well as in the production and repair of road surfaces. For example, researchers at the Massachusetts Institute of

Suggested Citation:
Gritsyuk V., Nevliudov I., Zablodskiy M., & Subramanian, P. (2022). Estimation of eddy currents and power losses in the rotor of a screw electrothermomechanical converter for additive manufacturing *Machinery & Energetics* 13(2), 41-49.

*Corresponding author

Technology in [8] presented a large-scale digital construction platform (DCP) for on-site sensing, analysis, and digital production. The second version of DCP used a tracked electric car as a platform and was used to extrude foam when pouring walls, which is similar to the block construction method. In [9], the authors developed a mobile printing system comprising two robotic manipulators on a mobile base that prints cement objects of a fairly large size. Researchers from the Institute of Advanced Architecture of Catalonia (IAAC) presented the idea of mobile 3D printing, where three separate systems are used to print architectural structures using cement [10].

According to the concept of "self-repairing cities" [11; 12], a fleet of autonomous vehicles and drones will scan roads for cracks and eliminate them before potholes appear. By detecting a crack in the road, a robot with a 3D printer will be able to place asphalt in the crack to repair it, all within a minute. This approach can be used at night to avoid road closures that can disrupt traffic. The device is based on the Mendel 90 desktop RepRap printer but is equipped with a special extruder and a nozzle made of high-temperature photopolymer. Printing is performed with bituminous crumb with millimetre-sized particles, which is poured into a hopper, heated, and pushed through a nozzle using an auger. The extruder assembly has an internal heating sleeve. The pellets soften as they pass through the auger, due to an increase in temperature under the action of heating resistors, which leads to the leakage of liquid bitumen from the nozzle, as demonstrated in Figure 1a. Stepper motors, temperature, gradient, and auger rotation speed are controlled by simple electronics connected to a PC (Fig. 1b). The improved mechanical properties are a function of temperature, which may be due to microstructural changes in asphalt. This leads to the formation of fibres that cover the cracks, which increases the impact strength. During experiments, the authors [11] found that a temperature between 125°C and 135°C is optimal for creating continuous asphalt extrusion with a constant line width.

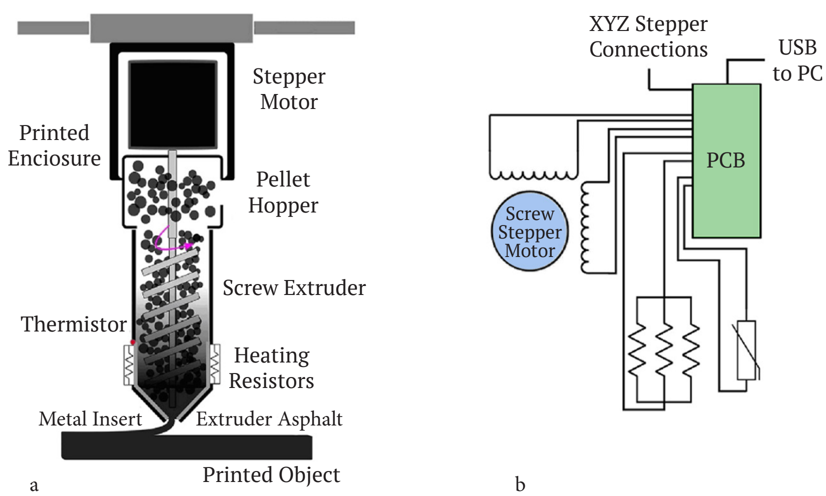

Figure 1. System design: extruder design (a), control electronics (b)

Source: [11]

The authors [11] believe that a fleet of autonomous vehicles will ensure the functioning of a new economic model underlying urban infrastructure that will help society. The improved and customisable properties of 3D-printed asphalt combined with the flexibility and efficiency of the platform will provide an advanced approach to the maintenance of urban infrastructure facilities.

Apart from roads, this will change the way hard-to-reach structures are repaired, such as flat roofs of buildings and other structures. The advantage of this method is not only the ability to reduce costs (other repair methods often require the construction of scaffolding and the closure or disconnection of infrastructure to gain access), but also the fact that repairs can be started earlier, before large-scale wear and tear occurs.

3D printing technology for large-scale structures can be improved by combining an electric motor, an auger extruder, and a heater in one housing. This will not only save weight and size, but also substantially increase the efficiency and reliability of the system due to functional integration and full use of the dissipative component of energy. The need for added heat sources will disappear, and the rotor-auger completely immersed in the material can transfer maximum thermal and mechanical energy to it.

The operability of the idea of combining an electric motor and a working body was demonstrated by the authors of the study [13], who showed the advantages of an energy-efficient industrial mixer for concrete production. The mixer is designed based on a synchronous electric motor with a massive rotor and permanent magnets. The mixing blades are installed directly on the shaft without gear transmission (Fig. 2). Devices of this design perform rotational and linear motion simultaneously and have a modular structure that can include any number of modules with a common three-phase winding [14-16]. As a rule, they are used for mixing and drilling [17; 18]; however, their potential applications range from machine tools to robotics and various devices used for assembly, gripping, moving, packing, shaking [15; 19].

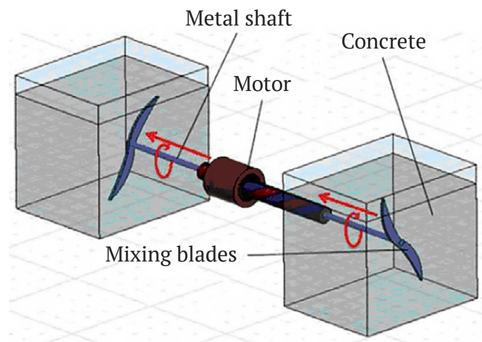

Figure 2. Design diagram of a permanent magnet motor

Source: [11]

For a clear comparison with the conventional electric motor used in industrial mixers, an asynchronous motor with equivalent mechanical power, rated rotational speed, and torque was chosen. The efficiency of a motor with a massive rotor and permanent magnets at full load is 94%, and the efficiency of an asynchronous motor is close to 87%.

The comparison is based on a paper presented at the conference on industrial and commercial energy use in 2013 [20]. Notably, the comparison of motors shown does not consider the heating losses of the massive rotor and stator, which should be used to heat and reduce the viscosity of the working medium [21; 22].

Therefore, to increase the efficiency, cost-effectiveness, and versatility of devices that provide transportation, mixing, pressing and heating operations, their use as links in the technological chain is important. As an alternative to the above approaches, a mobile robotic platform equipped with an auger-type electrothermomechanical converter (ETMC) is proposed. The proposed converter uses an external auger rotor, which simultaneously performs the functions of an asynchronous motor rotor, a heating element, an executive mechanism, and a protective housing (Fig. 3). Therefore, considering the "useful" losses of the electromagnetic system, the efficiency of electromechanical converters for technological purposes increases to 98-99% [23].

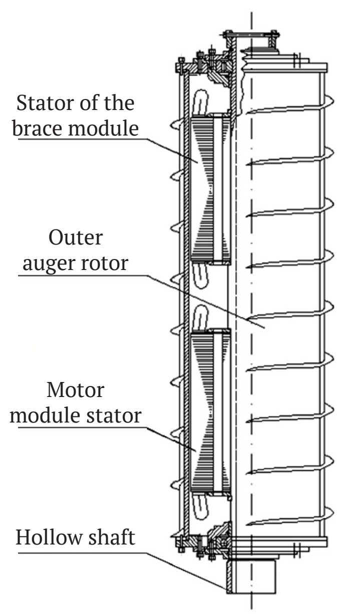

Figure 3. Design diagram of an auger-type ETMC

The auger-type ETMC uses the principle of self-regulation in energy conversion, according to which the distribution of thermal and mechanical energy into useful flows is carried out according to the value of the current slip, which depends on the ratio of electromagnetic moments of the engine and brake modules of the ETMC. When the stator winding of the motor module is connected to a voltage source, a rotating magnetic field is created, under the action of which eddy currents (EC) are induced in the adjacent zone of the external ferromagnetic rotor. As a result, an asynchronous electromagnetic moment is formed. The main mode can be considered the opposite direction of rotation of the fields, wherein the brake module works upon sliding $S_G>1$, i.e., in the mode of electromagnetic braking.

The study of the distribution of EC induced in electrically conductive media is of practical interest for a wide range of industrial applications. EC in vacuum chambers, cores of high-speed magnets and accelerating resonators cause many adverse effects. This primarily refers to heating the cores and electrically conductive structural elements and, accordingly, reducing the overall efficiency of the devices. At the same time, the assessment of the heat output that occurs in the conductors during the BC leak is important for various devices, such as induction furnaces, melting devices, soldering devices, etc. Especially relevant is the use of field calculation methods for electromechanical converters operating in difficult conditions. During the electromechanical conversion of energy into ETMC, a single physical force field occurs, the separate components of which are the fields of electromagnetic, thermal, and mechanical quantities.

Purpose of the study. For a preliminary assessment of the efficiency of using auger-type ETMCS as part of mobile robotic platforms for industrial 3D printing, it is necessary to analyse the distribution of EC in the ferromagnetic rotor as the main sources of heat generation. This will serve as important information for predicting the optimal temperature, gradient, and rotation speed of the auger extruder. In turn, these values will determine the mechanical properties of the material at the output of the device.

MATERIALS AND METHODS

When developing an auger-type ETMC, it is necessary to perform a quantitative analysis of the distribution of the EC density and the power density that is dissipated, to develop recommendations for choosing rational parameters and heating modes of the material. Conventional methods and approaches to calculating and analysing processes in ETMC, due to the specificity of functioning, do not provide the necessary reliability of the results. Methods that ensure high reliability of calculations are field and circle-field methods of analysis, which are invariant to the nature of electromagnetic connections of the object of research, consider the real geometry and properties of materials. Circle-field methods are used in the analysis of dynamic operating modes of electromechanical converters. The use of the field analysis method allows conducting refined studies of the parameters, characteristics, and operating modes of the ETMC, considering the design features and operating modes that do not lend themselves to reliable analysis by conventional, classical methods.

In the study of electromechanical converters, numerical methods for calculating the field are widely used, considering the features of the geometry and saturation of cores, among which the finite element method is particularly progressive. According to the finite element method, the study area is divided into sections. The solution of differential equations is reduced to solving a system of algebra equations that relate the values of the vector field potential at nodal points, obtained by dividing into sections. The method of conduction of toothed contours has become widespread, according to which the complete field of the machine is considered, taking into account its change in time during the mutual movement of the toothed cores. Electromagnetic processes are calculated by jointly solving a system of differential equations written in matrix form for the circuits of an electrical circuit that includes machine windings and external electrical circuits.

The highest accuracy of analysis is provided upon calculating a three-dimensional problem. This becomes possible when considering the majority of physical effects, which are more deeply manifested in conditions of full reproduction of the geometry of the device. The solution of a system of equations describing a three-dimensional electromagnetic and temperature field at any given time for any spatial point in the model can only be implemented by numerical methods. These methods are widely used in modern multiphysical modelling software packages Cedrat Flux, Comsol Multiphysics, Ansys, etc.

To fulfil this purpose, the mathematical model presented in [24; 25] was used. In this study, a three-dimensional modification of the finite-element model, implemented within the Comsol Multiphysics software and computing complex, has been implemented. Means of analysing the results of calculations of this particular complex allow obtaining comprehensive information about the processes that take place in the object under study. Therewith, Comsol Multiphysics is one of the most proven and affordable software products that implement the finite element method.

Calculation of the three-dimensional distribution of the EC was performed on the rotor section for the engine module of the experimental sample of the auger-type ETMC. The three-dimensional geometry of the model comprises the following design sections: a hollow external rotor, a toothed stator magnetic circuit, an air gap, and a stator winding. The angular velocity of the rotor is defined as the frequency of field sources according to the rotor coordinate system. The specific electrical conductivity of the rotor material was taken according to the reference data, considering the average temperature at the operating sliding of the engine module S=0.88. The nonlinearity of the magnetic properties of the massive rotor and stator core is considered by setting the corresponding magnetisation curves. Field sources are set by an extraneous current density in the sections of the stator grooves according to the three-phase winding connection scheme

RESULTS AND DISCUSSION

The result of solving the field problem in the form of a three-dimensional distribution of EC is presented in Figure 4. A single cross-section of a hollow rotor is given for a slip value of S=0.88 (n^2=90 rpm). The section is made in the "edge" zone of the hollow cylinder, and the value of the z-component of the density of the EC is determined by colouring it in different colours and intensities. The same figure shows the line along which the section of the rotor wall is made, presented in Figure 5.

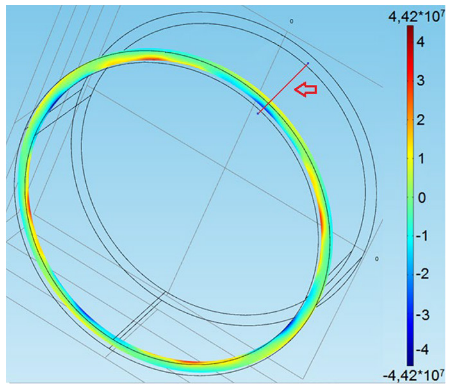

Figure 4. Distribution of the z-component of the EC density in the cross-section of the outer hollow rotor at *S*=0.88 (A/m^2)

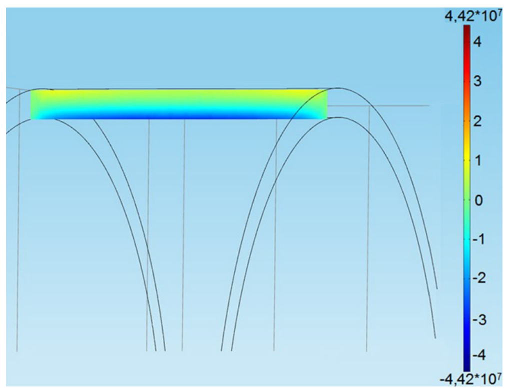

Figure 5. Distribution of the z-component of the EC density in the wall of the outer hollow rotor at *S*=0.88 (A/m^2)

The largest value of the normal component of the EC density slightly exceeds the maximum value (4.42 A/mm^2) of the z-component for *S*=0.88. On the three-dimensional picture of the distribution of the normal component (Fig. 6), internal areas of high density of EC are visible, which are conditioned upon the presence of the internal toothed-groove structure of the stator. That is, the main source of heat output is a layer of the inner surface of the rotor (4-5 mm), facing the source of the electromagnetic field.

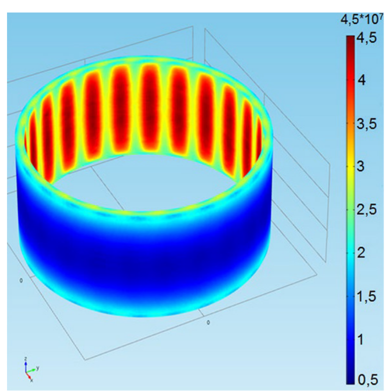

Figure 6. Distribution of the normal component of the EC density in the outer hollow rotor at *S*=0.88 (A/m^2)

The pattern of distribution of the dissipated power density, which considers all types of losses in the rotor, has a similar nature (Fig. 7). Preferably, the density of dissipated power on the outer surface of the rotor is within (10.5-20)·10^6 W/m^3. A considerable difference in the dissipated power density between the inner and outer surfaces of the rotor under operating conditions is not critical. The thermal energy of the rotor is actively transferred to the surrounding material, and the temperature gradient towards the cylinder wall thickness will stay small [22].

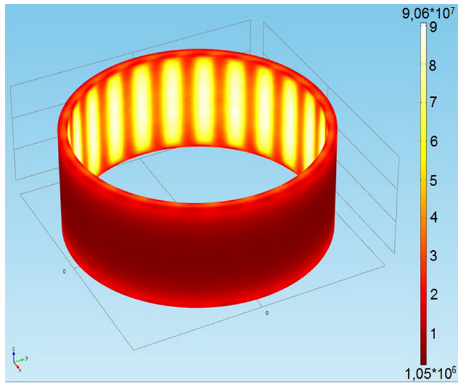

Figure 7. Distribution of the power density dissipated in the external hollow rotor at *S*=0.88 (W/m^3)

Note that the nature of the distribution of the dissipated power density in the rotor changes substantially with increasing field frequency, which affects the quality of thermal action on the material. This is conditioned upon a change in the configuration of the EC flow contours, probably due to a decrease in the depth of penetration of the electromagnetic field, as well as the influence of the edge effect.

The considerable scientific achievements of foreign authors in the field of research of electromagnetic and thermal processes in converters should be noted, which are the closest in terms of the ideology of creation. A sizeable number of publications investigate the physical fields in the core of electromechanical transducers with a ferromagnetic rotor using numerical methods. Thus, the authors of [26] performed a three-dimensional calculation of the finite element model of a rotational-linear converter, considering transients in the active part. The authors of studies [27-29] presented the analysis of the spiral motion engine using the method of Fourier series, which considers edge effects, the authors [30; 31] developed a technique for determining the parameters of the equivalent circuit of substitution, despite the small magnetisation inductance of the structure of the secondary conductive sleeve. In [32], a three-dimensional finite element analysis of a rotational linear motor is presented, which considers the longitudinal and transverse edge effects, the surface effect, and the influence of the thickness of the extreme sheets of a magnetic circuit. The study [33] contains simulation results for a two-module motor with an external rotor, namely the influence of the electric motor design on the torque and its pulsation is analysed. Calculations allow finding the electromechanical parameters for a particular engine that is being designed. In contrast to the above studies, this paper contains the results of calculating the three-dimensional distribution of eddy currents and the density of dissipated power, namely for an external ferromagnetic rotor. Furthermore, the calculation is performed considering the "useful" heat losses of the rotor used to heat the material. That is, the available electromechanical converters do not use the heating losses of the rotor and stator to heat and melt the working medium.

CONCLUSIONS

Additive manufacturing has enormous potential in the construction industry, as well as in the production and repair of road surfaces. Mobile platforms for 3D printing can solve the problem of limited workspace. To increase the efficiency and cost-effectiveness of the mobile robotic platform for 3D printing technology of large-scale structures, it is proposed to improve the design of the extruder assembly. This is achieved by combining an electric motor, auger extruder, and heater in one housing. This approach saves weight and size, as well as substantially increases the efficiency and reliability of the system due to functional integration and full use of the dissipative component of energy.

The proposed converter for a mobile robotics platform uses an external auger rotor, which simultaneously performs the functions of an asynchronous motor rotor, a heating element, an executive mechanism, and a protective housing. To pre-evaluate the efficiency of using an auger-type ETMC as part of a mobile robotic platform for industrial 3D printing, a finite element calculation of the spatial distribution of the EC in the hollow rotor section was performed for the motor module of an experimental sample of an auger-type ETMC. Estimating the levels of dissipated power density on the rotor surface allows discussing the prospects of the proposed approach for optimising the design of the extruder assembly of a mobile robotic platform for industrial 3D printing. The results of the spatial distribution of the rotor EC will allow improving the design of the ETMC, to ensure the set values of temperature and gradient, which determine the mechanical properties of the material at the output of the device.

Further research in this area should be a physical experiment, as well as a detailed analysis of the spatial configuration of contours B due to the direct impact on the quality of heat treatment of the material.

REFERENCES

[1] Katz-Demyanetz, A., Popov, V.V.Jr, Kovalevsky, A., Safranchik, D., & Koptyug, A. (2019). Powder-bed additive manufacturing for aerospace application: Techniques, metallic and metal/ceramic composite materials and trends. *Manufacturing Revew*, 6, article number 5.

[2] Yuk, H., Lu, B., Qu, K., Xu, J., Zhao, X., Lin, S., & Luo, J. (2020). 3D printing of conducting polymers. *Nature Communications*, 11, article number 1604. doi: 10.1038/s41467-020-15316-7.

[3] Birbara, N.S., Otton, J.M., & Pather, N. (2017). 3D modelling and printing technology to produce patient-specific 3D models. *Heart Lung Circulation*, 28(2), 302-313. doi: 10.1016/j.hlc.2017.10.017.

[4] Jankovics, D. (2019).Customization of automotive structural components using additive manufacturing and topology optimization. *IFAC-PapersOnLine*, 52(10), 212-217. doi: 10.1016/j.ifacol.2019.10.066.

[5] Kolomiets, A., Grobman, Y.J., Popov, Jr.V.V., Strokin, E., Senchikhin, G., & Tarazi, E. (2020). The titanium 3D printed flute: New prospects of additive manufacturing for musical wind instruments design. *Journal of New Music Research*, 50(1), 1-17. doi: 10.1080/09298215.2020.1824240.

[6] Wohlers, T.T., Campbell, I., Diegel, O., Huff, R., & Kowen, J. (2021). *Wohlers report 2020: 3D printing and additive manufacturing state of the industry*. Fort Collins: Wohlers Associates.

[7] Sauter, A., Nasirov, A., Fidan, I., Allen, M., Elliott, A., Cossette, M., & Singer, T. (2021). Development, implementation and optimization of a mobile 3D printing platform. *Progress in Additive Manufacturing*, 6(2), 231-241. doi: 10.1007/s40964-020-00154-2.

[8] Keating, S, Spielberg, N.A., Klein, J, & Oxman, N. (2014). A compound arm approach. In *Robotic Fabrication in Architecture* (pp. 99-110). Dordrecht: Springer. doi: 10.1007/978-3-319-04663-1_7.

[9] Efe Tiryaki, M., Zhang, X., & Pham, Q.C. (2018). Printing-while-moving: A new paradigm for large-scale robotic 3D Printing. *IEEE International Workshop on Intelligent Robots and Systems*, 4, 2286-2291. doi: 10.1109/IROS40897.2019.8967524.

[10] Hall, N. (2016). *IAAC Minibuilders small robots with big ambitions. 3D Print Ind, WA*. Retrieved from https://3dprintingindustry.com/news/iaac-minibuilders-small-robots-big-ambitions-83257/.

[11] Jackson, R.J., Wojcik, A., & Miodownik, M. (2018). 3D printing of asphalt and its effect on mechanical properties. *Materials & Design*, 160, 468-474. doi: 10.1016/j.matdes.2018.09.030.

[12] Johansson, A. (2016). *3D printing robot may be the solution to potholes, PSFK*. Retrieved from https://www.psfk.com/print-post?format=pdf&id=322046.

[13] Dobzhanskyi, O., Amiri, E., & Gouws, R. (2016). Comparison analysis of electric motors with two degrees of mechanical freedom: PM synchronous motor vs induction motor. In *II International Young Scientists Forum on Applied Physics and Engineering* (pp. 14-17). Kharkiv: Kharkiv National Agrarian University named after V.V. Dokuchaiev. doi: 10.1109/YSF.2016.7753750.

[14] Alwash, J.H., & Qaseer L.J. (2010). Three-dimension finite element analysis of a helical motion induction motor. *ACES*, 25(8), 703-712.

[15] Bolognesi, P. (2010). A novel rotary-linear permanent magnets synchronous machine using common active parts. In *15th IEEE Mediterranean Electrotechnical Conference* (pp. 1179-1183). Valletta: The University of Malta. doi: 10.1109/MELCON.2010.5476370.

[16] Bentia, I., & Szabo, L. (2010). Rotary-linear machines – A survey. *Journal of Computer Science and Control Systems*, 3, 11-14.

[17] Zhao, J., Liu, X., Xin, Z. & Han, Y. (2009). Research on the energy-saving technology of concrete mixer trucks. In *4th IEEE Conference on Industrial Electronics and Applications* (pp. 3551-3554). Xi'an: Xi'an University of Science and Technology.

[18] Szczygieł, M., & Kluszczyński, K. (2016). Rotary-linear induction motor based on the standard 3-phase squirrel cage induction motor – constructional and technological features. *Czasopismo Techniczne. Elektrotechnika*, 1, 395-406. doi: 10.4467/2353737XCT.15.059.3859.

[19] Bolognesi, P., Bruno, O., Landi, A., Sani, L., & Taponecco L. (2004). Electromagnetic actuators featuring multiple degrees of freedom: A survey. In *16th International Conference on Electrical Machines – ICEM 2004* (pp. 1-6). Cracow: Cracow University of Technology.

[20] Dobzhanskyi, O., & Gouws, R. (2017). 3-D Finite element method analysis of twin-armature permanent magnet motor with two degrees of mechanical freedom. *Springer Electrical Engineering*, 99(3), 997-1004.

[21] Zablodskiy, M., Zhiltsov, A., Kondratenko, I., & Gritsyuk, V. (2017). Conception of efficiency of heat electromechanical complex as hybrid system. Electrical and Computer Engineering (UKRCON). In *2017 IEEE First Ukraine Conference* (pp. 399-404). Kyiv: Taras Shevchenko National University of Kyiv. doi: 10.1109/UKRCON.2017.8100519.

[22] Zablodskiy, N., Pliugin, V., & Gritsyuk, V. (2014). Submersible electromechanical transformers for energy efficient technologies of oil extraction. *Progressive Technologies of Coal, Coalbed Methane, and Ores Mining*, 9, 223-227.

[23] Zablodskii, N.N., Plyugin, V.E., Gritsyuk, V.Y., & Grin, G.M. (2016). Polyfunctional electromechanical energy transformers for technological purposes. *Russian Electrical Engineering*, 87, 140-144. doi: 10.3103/S1068371216030123.

[24] Zablodskiy, M., Gritsyuk, V., Rudnev, Y., & Brozhko, R. (2019). Three-dimensional electromagnetic field model of an auger electromechanical converter with an external solid rotor. *Mining of Mineral Deposits*, 13(4), 99-106. doi: 10.33271/mining13.04.099.

[25] Zablodskiy, M., Gritsyuk, V., Rudnev, Y., Brozhko, R., & Tymofieieva, O. (2020). Analysis of 3D eddy current distribution in a hollow rotor of an electromechanical converter. In *IEEE 40th International Conference on Electronics and Nanotechnology* (pp. 561-564). Kyiv: Taras Shevchenko National University of Kyiv. doi: 10.1109/ELNANO50318.2020.9088777.

[26] Amiri, E. (2014). Circuit modeling of double-armature rotary-linear induction motor. In *IECON 2014-40th annual conference of the IEEE industrial electronics society* (pp. 431-436). Dallas: Dallas Theological Seminary.

[27] Mendrela, E.A., & Turowski, J. (1978). Rotary-linear induction motor. In *IEEE winter power meeting* (article number A78091-1). New York: Columbia University.

[28] Fleszar, J., & Mendrela, E.A. (1983). Twin-armature rotarylinear induction motor. *IEE Proceedings B (Electric Power Applications)*, 130(3), 186-192.

[29] Mendrela, E.A., & Geirczak, E. (1987). Double-winding rotary-linear induction motors. *IEEE Transactions on Energy Conversion*, EC–2(1), 48-54.

[30] Cathey, J.J. (1985). Helical motion induction motor. *Proceedings of the Institution of Electrical Engineers*, 132(2), 112-114.

[31] Rabiee, M., & Cathey, J.J. (1988). Verification of a field theory analysis applied to a helical motion induction motors. *IEEE Transactions on Magnetics*, 24(4), 127-138.

[32] Alwash, J.H., & Qaseer, L.J. (2010). Three-dimension finite element analysis of a helical motion induction motor. *Applied Computational Electromagnetics Society Journal*, 25(8), 703-712.

[33] Łukaniszyn, M., Kowol M., & Kołodziej, J. (2010). Performance analysis of a two-module reluctance motor with an axial flux. *Computer Applications in Electrical Engineering*, 8, 72-80.

СПИСОК ВИКОРИСТАНИХ ДЖЕРЕЛ

[1] Powder-bed additive manufacturing for aerospace application: Techniques, metallic and metal/ceramic composite materials and trends / A. Katz-Demyanetz et al. *Manufacturing Revew*. 2019. Vol. 6. Article number 5.

[2] 3D printing of conducting polymers / H. Yuk et al. *Natural Communication*. 2020. Vol. 11. Article number 1604. doi: 10.1038/s41467-020-15316-7.

[3] Birbara N.S., Otton J.M., Pather N. 3D modelling and printing technology to produce patient-specific 3D models. *Heart Lung Circulation*. 2019. Vol. 28, No. 2. P. 302–313. doi: 10.1016/j.hlc.2017.10.017.

[4] Jankovics D. Customization of automotive structural components using additive manufacturing and topology optimization. *IFAC-PapersOnLine*. 2019. Vol. 52, No 10. P. 212–217. doi: 10.1016/j.ifacol.2019.10.066.

[5] The titanium 3D printed flute: New prospects of additive manufacturing for musical wind instruments design / A. Kolomiets et al. *Journal of New Music Research*. 2020. Vol. 50, No. 1. P. 1–17. doi: 10.1080/09298215.2020.1824240.

[6] Wohlers report 2020: 3D printing and additive manufacturing state of the industry / T.T. Wohlers et al. Fort Collins: Wohlers Associates, 2021. 374 p.

[7] Development, implementation and optimization of a mobile 3D printing platform / A. Sauter et al. *Progress in additive manufacturing*. 2021. Vol. 6, No. 2. P. 231–241. doi: 10.1007/s40964-020-00154-2.

[8] Keating S, Spielberg N.A., Klein J, Oxman N. A compound arm approach. *Robotic Fabrication in Architecture*. Dordrecht: Springer, 2014. P. 99–110. doi: 10.1007/978-3-319-04663-1_7.

[9] Efe Tiryaki M., Zhang X., Pham Q.C. Printing-while-moving: A new paradigm for large-scale robotic 3D Printing. *IEEE International Workshop on Intelligent Robots and Systems*. 2018. Vol. 4. P. 2286–2291. doi: 10.1109/IROS40897.2019.8967524.

[10] Hall N. IAAC Minibuilders small robots with big ambitions. 3D Print Ind, WA. URL: https://3dprintingindustry.com/news/iaac-minibuilders-small-robots-big-ambitions-83257/.

[11] Jackson R.J., Wojcik A., Miodownik M. 3D printing of asphalt and its effect on mechanical properties. *Materials & Design*. 2018. Vol. 160. P. 468–474. doi: 10.1016/j.matdes.2018.09.030.

[12] Johansson A. 3D printing robot may be the solution to potholes, PSFK. URL: https://www.psfk.com/print-post?format=pdf&id=322046.

[13] Dobzhanskyi O., Amiri E., Gouws R. Comparison analysis of electric motors with two degrees of mechanical freedom: PM synchronous motor vs induction motor. *II international young scientists forum on applied physics and engineering* (Kharkiv, 10-14 Oct. 2016). Kharkiv, 2016. P. 14–17. doi: 10.1109/YSF.2016.7753750.

[14] Alwash J.H., Qaseer L.J. Three-dimension finite element analysis of a helical motion induction motor. *ACES*. 2010. Vol. 25, No 8. P. 703–712.

[15] Bolognesi P. A novel rotary-linear permanent magnets synchronous machine using common active parts. *15th IEEE Mediterranean Electrotechnical Conference*. (Valletta, 26–28 April 2010). Valletta, 2010. P. 1179–1183. doi: 10.1109/MELCON.2010.5476370.

[16] Bentia I., Szabo L. Rotary-linear machines – A survey. *Journal of Computer Science and Control Systems*. 2010. Vol. 3. P. 11–14.

[17] Zhao J., Liu X., Xin Z., Han Y. Research on the energy-saving technology of concrete mixer trucks. *4th IEEE Conference on Industrial Electronics and Applications*. (Xi'an, 25-27 May 2009). Xi'an, 2009. P. 3551–3554.

[18] Szczygieł M., Kluszczyński K. Rotary-linear induction motor based on the standard 3-phase squirrel cage induction motor – constructional and technological features. *Czasopismo Techniczne. Elektrotechnika*. 2016. Vol. 1. 395–406. doi: 10.4467/2353737XCT.15.059.3859.

[19] Electromagnetic actuators featuring multiple degrees of freedom: A survey / P. Bolognesi et al. *16th International Conference on Electrical Machines – ICEM 2004*. (Cracow, 20–25 May 2004). Cracow, 2004. P. 1–6.

[20] Dobzhanskyi O., Gouws R. 3-D Finite element method analysis of twin-armature permanent magnet motor with two degrees of mechanical freedom. *Springer Electrical Engineering*. 2017. Vol. 99, No. 3. P. 997–1004.

[21] Zablodskiy M., Zhiltsov A., Kondratenko I., Gritsyuk V. Conception of efficiency of heat electromechanical complex as hybrid system. Electrical and Computer Engineering (UKRCON). *2017 IEEE First Ukraine Conference*. (Kyiv, 29 May–2 June 2017). Kyiv, 2017. P. 399–404. doi: 10.1109/UKRCON.2017.8100519.

[22] Zablodskiy N., Pliugin V., Gritsyuk V. Submersible electromechanical transformers for energy efficient technologies of oil extraction. *Progressive Technologies of Coal, Coalbed Methane, and Ores Mining*. 2014. Vol. 9. P. 223–227.
[23] Zablodskii N.N., Plyugin V.E., Gritsyuk V.Y., Grin G.M. Polyfunctional electromechanical energy transformers for technological purposes. *Russian Electrical Engineering*. 2016. Vol. 87. P. 140–144. doi: 10.3103/S1068371216030123.
[24] Zablodskiy M., Gritsyuk V., Rudnev Y., Brozhko R. Three-dimensional electromagnetic field model of an auger electromechanical converter with an external solid rotor. *Mining of Mineral Deposits*. 2019. Vol. 13, No. 4. P. 99–106. doi: 10.33271/mining13.04.099.
[25] Analysis of 3D eddy current distribution in a hollow rotor of an electromechanical converter / M. Zablodskiy et al. *IEEE 40th International Conference on Electronics and Nanotechnology*. (Kyiv, 22–24 April 2020). Kyiv, 2020. P. 561–564. doi: 10.1109/ELNANO50318.2020.9088777.
[26] Amiri E. Circuit modeling of double-armature rotary-linear induction motor. *IECON 2014–40th Annual Conference of the IEEE Industrial Electronics Society* (Dallas, 29 Oct.–1 Nov. 2017). Dallas, 2014. C. 431–436.
[27] Mendrela E.A., Turowski J. Rotary-linear induction motor. *IEEE winter power meeting* (New York, 29 Jan–3 Feb. 1978). New York, 1978. Article number A78091-1.
[28] Fleszar J., Mendrela E.A. Twin-armature rotarylinear induction motor. *IEEE proceedings B (electric power applications)*. 1983. Vol. 130, No. 3. P. 186–192.
[29] Mendrela E.A., Geirczak E. Double-winding rotary-linear induction motors. *IEEE transactions on energy conversion*. 1987. Vol. EC–2, No. 1. P. 48–54.
[30] Cathey J.J. Helical motion induction motor. *Proceedings of the Institution of Electrical Engineers*. 1985. Vol. 132, No. 2. P. 112–114.
[31] Rabiee M., Cathey J.J. Verification of a field theory analysis applied to a helical motion induction motors. *IEEE transactions on magnetics*. 1988. Vol. 24, No. 4. P. 127–138.
[32] Alwash J.H., Qaseer L.J. Three-dimension finite element analysis of a helical motion induction motor. *Applied Computational Electromagnetics Society Journal*. 2010. Vol. 25, No. 8. P. 703–712.
[33] Łukaniszyn M., Kowol M., Kołodziej J. Performance analysis of a two-module reluctance motor with an axial flux. *Computer Applications in Electrical Engineering*. 2010. Vol. 8. P. 72–80.

Володимир Юрійович Грицюк[1], Ігор Шакирович Невлюдов[1], Микола Миколайович Заблодський[2], Періасамі Субраманіан[3]

[1]Харківський національний університет радіоелектроніки
61166, просп. Науки, 14, м. Харків, Україна

[2]Національний університет біоресурсів і природокористування України
03041, вул. Героїв Оборони, 15, м. Київ, Україна

[3]Державний аграрний університет Таміл Наду
641003, Лоулі Роуд, м. Коімбатур, Індія

Оцінка вихрових струмів і втрат потужності у роторі шнекового електротепломеханічного перетворювача для адитивного виробництва

Анотація. Технології 3D-друку великомасштабних структур дозволяють архітекторам і будівельникам значно розширити межі проектування конструкцій та підвищити ефективність їх будівництва. Мобільні робототехнічні платформи для 3D-друку все частіше впроваджуються в будівельній сфері, а також при виробництві дорожніх покриттів, дозволяючи вирішити проблему обмеженого робочого простору. Типова конструкція вузла екструдера робототехнічної платформи для 3D-друку великомасштабних структур може бути вдосконалена шляхом об'єднання електродвигуна, шнекового екструдера та нагрівача в одному корпусі. Пропонований шнековий електротепломеханічний перетворювач використовує зовнішній ротор-шнек, який одночасно виконує функції ротора асинхронного двигуна, нагрівального елемента, виконавчого механізму і захисного корпусу. Метою статті є оцінка ефективності використання шнекового перетворювача у складі мобільної робототехнічної платформи для адитивного виробництва. Для перетворювачів, які функціонують в складних умовах, актуальним є застосування польових методів розрахунку. В роботі проведено польовий розрахунок методом кінцевих елементів та визначено просторовий розподіл вихрових струмів на ділянці порожнистого феромагнітного ротора. Із використанням програмно-обчислювального комплексу Comsol Multiphysics отримано картини тривимірного розподілу z-складової, нормальної складової густини вихрових струмів, а також розподілу густини дисипованої потужності, що враховує всі види втрат в роторі. Практичне значення отриманих результатів полягає в можливості прогнозування оптимальних показників впливу теплового режиму на матеріал, а також швидкості обертання ротора перетворювача. Це в свою чергу, буде визначати механічні властивості матеріалу на виході пристрою

Ключові слова: 3D-друк, мобільна робототехнічна платформа, чисельний розрахунок, зовнішній шнековий ротор, вузол екструдера, густина потужності